


ORIGINAL ARTICLE

Open Access



Removal efficiency of restroom ventilation revisited for short-term evaluation

Yuyao Chen¹, Zhiqiang Zhai², Zhe Yuan¹ and Guoqing He^{1*} 

*Correspondence:
Guoqinghe@zju.edu.cn

¹ College of Civil Engineering and Architecture, Zhejiang University, Hangzhou, China

² Department of Civil, Environmental and Architectural Engineering, University of Colorado at Boulder, Colorado, USA

Abstract

Ventilation efficiency or contaminant removal efficiency is often evaluated using the ratio between the concentrations in the exhaust air and the room air. This ratio does not truly represent the expectation of ventilation in restrooms, where dynamic airflow fields and sources are more typical. This study focuses on a short-term (10 min) pollutant removal percentage in a residential restroom featuring a dynamic airflow field, particularly with the onset of window-induced stack ventilation during toilet uses. Thirteen ventilation scenarios of a residential restroom were studied using the numerical method that was validated by a mock-up experiment. The scenarios differed in the operation of the exhaust fan and window. Results show that the 10-min pollutant removal percentage of a typical exhaust ventilation system at 10 h⁻¹ air change rate (ACH) is only 68.5%. Under exhaust ventilation, opening the window can introduce both adverse short circuit and favorable stack ventilation depending on the difference between the indoor and outdoor temperatures. As the temperature difference increases from 0 to 12.5 °C, the removal percentage increases from below 50%, a drop due to short circuit, to above 98% thanks to a tripled ventilation rate. The human thermal plume has notable effect on the removal percentage, but its effect can be neglected with the presence of stack ventilation. The hybrid ventilation strategy has impact on perceived air quality and thermal comfort. When the outdoor air is colder, opening the window under exhaust ventilation may increase the current sitting user's exposure to the self-produced pollutants but can reduce the exposure of the next immediate standing user. In addition, opening the window in cold days will make the toilet user thermally uncomfortable with reduced local temperatures and increased airflow velocities. The study highlights the importance of using the short-term removal percentage to evaluate the performance of restroom ventilation.

Keywords: Removal percentage, Stack ventilation, Residential restroom, Hybrid ventilation, CFD

Introduction

Indoor air quality (IAQ) is important to the health and well-being of occupants (Rueda López et al. 2021; WHO 2010). Despite the large amount of IAQ studies on indoor spaces in general, some specific spaces have been paid less attention, such as garages, attics, or basements. One of such spaces is the restroom space. Restrooms

are large in number and are among the most frequently used indoor spaces in a person's daily life. In addition to unpleasant odorous gaseous pollutants (Sato et al. 2002), restrooms are also potential sources of bioaerosol contaminants (Gerba et al. 1975). In the recent worldwide pandemic, many restrooms were found heavily contaminated with bacteria and viruses (Dancer et al. 2021; Ding et al. 2020; Hu et al. 2020). These types of pathogens, mostly resulted from the vomit and excrement of virus-infected persons (Chen et al. 2020), can survive for a long time in the restroom environment (Johnson et al. 2013). Toilet flushing and hand washing actions produce droplet nuclei that can carry these pathogens into the air (Ali et al. 2022; Barker and Jones 2005; Luo et al. 2023). Subsequent infection can occur if these airborne pathogens are not disinfected or removed by the ventilation system (Cai et al. 2020; Cao et al. 2022; Lee and Tham 2021; Wang and Liu 2021).

Ventilation remains as an effective control measure to remove indoor pollutants (ASHRAE 2019). Ventilation rates have a significant impact on human health (Aganovic et al. 2021; Wargocki et al. 2002). Efficient pollutant removal is a major concern of the ventilation design in restrooms (Lin 2021; Seo and Seouk Park 2013; Yang and Kim 2017). Existing building standards have prescribed minimal ventilation rates for restrooms. ASHRAE 62.1 specifies a low rate and a high rate of 25 L/s and 35 L/s, respectively, per toilet fixture for public restrooms and 12.5 L/s and 25 L/s for private restrooms (ASHRAE 2019). Chinese standards GB50736-2012 requires an air change rate (ACH) of 5 h^{-1} to 10 h^{-1} in public restrooms and no less than 3 h^{-1} in residential restrooms (MOHURD 2012).

In addition to ventilation rates, ventilation designs also specify a ventilation scheme with proper ventilation effectiveness, which is strongly dependent on inlet/outlet positions and source locations (Cetin et al. 2020). For gaseous contaminant removal, the relative source positions in the dominant airflow path created by the ventilation system are important (He et al. 2005). This could also be true for the removal of bioaerosols or fine particles ($<1 \mu\text{m}$) (Liu et al. 2023; Rim and Novoselac 2010; Zhao and Wu 2009). In restrooms, an ideal ventilation system should have exhaust fans placed as close as possible to the source (Mui et al. 2017; J.-X. Wang et al. 2022a, b; Zhang et al. 2022). Removal efficiency, an indicator for the quality of supply air distribution in ventilated rooms, has been used to quantify the efficiency of ventilation systems in restroom spaces (Cetin et al. 2020; Fisk et al. 1997; Tung et al. 2010). However, whether this efficiency is sufficient for the ventilation performance evaluation in restrooms is debatable. Removal efficiency, based on the ratio of the exhaust concentration to the supply concentration, indicates how well the space is ventilated compared with the perfect mixing condition. It does not tell how fast the space returns to its background concentration level after an instant release of contaminants. In restrooms, it is more common to see instant releases of contaminants, such as toilet uses for feces and urine releasing (Tung et al. 2009), aerosol antiperspirant spraying (Seller et al. 2021), etc. Restrooms in fact require an efficient removal of odor in a short time frame because of the nature of usage. And in the case of pathogen transmissions, cross-infections can occur in a very short time. In one reported case, the COVID-19 infection occurred after the infected person spent only 14 seconds with the carrier in a public restroom (Zhang 2021). This evidence suggests the importance of the often-neglected time factor in ventilation efficiency. In such a short time,

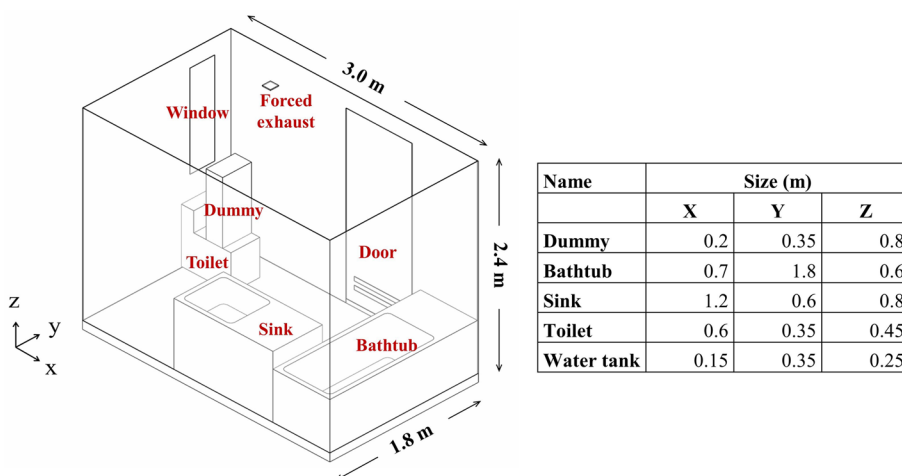


Fig. 1 Configuration of the model restroom

the dynamic performance of ventilation is of more interest than a steady state performance. Therefore, restroom ventilation needs to be revisited.

Compared to public restrooms, residential restrooms receive less attention and are held to lower ventilation standards. The role of residential restrooms in family transmission and community transmission during pandemic are by no means less important, as suggested by studies on the 2003 SARS outbreak in Hong Kong’s Amoy Gardens apartment complex (Yu Ignatius T.S. et al. 2004) or recent multiple community outbreaks of COVID-19 in Hong Kong (Q. Wang et al. 2022a, b), Guangzhou (Kang et al. 2020), and Seoul (Hwang et al. 2021). In China, residential restrooms usually have a window that opens to the outside, giving users the option to induce natural ventilation. Cold airflows from windows can significantly affect indoor airflow patterns (Ameen et al. 2019) and contaminant concentrations (Seller et al. 2021). However, few studies have explored the impact of window-induced stack ventilation on contaminant removal rates.

In this paper, we consider the factor of window opening and examine how window-induced stack ventilation affects the removal rate of gaseous pollutants released during the toilet usage. The results may also apply to certain fine airborne pathogen-containing nuclei as these fine particles (< 1 μm) have similar aerodynamics in built environment (Ai et al. 2020; Rim and Novoselac 2010). The dynamic ventilation performance is evaluated using the Computational Fluid Dynamics (CFD) method. The study is to answer 1) whether the common exhaust ventilation system is efficient in removing the pollutants, 2) whether opening the window helps remove pollutants, and 3) what the impact of the toilet user’s thermal plume is on the pollutant removal.

Methods

Room configuration

The restroom under investigation had an internal dimension of 3.00 m (length)×1.80 m (width)×2.40 m (height) as shown in Fig. 1. Four boxes of different sizes were used to model a bathtub, a toilet, a cabin counter, and a sitting person. The ventilation system was composed of a ceiling exhaust, a window, a door seam, and a door vent. The ceiling

exhaust (0.10 m × 0.10 m) and the window (0.35 m × 1.30 m) were both close to the toilet. The door vents were two identical openings (0.6 m × 0.05 m) at the bottom part. The door seam, when considered, had a dimension of 0.80 m × 0.05 m. The ceiling exhaust was 0.83 m from the wall with the window and 0.55 m from the wall with the door. To simulate the odorous pollutants generated during the toilet usage, an area source (0.10 m × 0.10 m) was located on top of the toilet box and right behind the sitting dummy.

CFD models

In the CFD models, all openings, if open, were set as zero pressure outlet. The exhaust was given a fixed airflow rate of 0.036 m³/s (10 h⁻¹ ACH). The indoor temperature was 23 °C. In the simulations involving stack ventilation, the surface temperatures of the walls and floor were 21 °C and remained constant. It was assumed that the changes in surface temperature were negligible within 10 minutes because of the thermal mass. In the simulations without stack ventilation, the surface temperatures of the walls and the floor were the same as that of the room. The human dummy was present in all simulations but was set to 32 °C (Cheng et al. 2020; Liu et al. 2022) only in cases when human thermal plume was activated. There was a lack of data on the releasing rates of odorous pollutants during toilet usages. A wide range of tracer gas emission rates (0.02 L/min to 0.30 L/min) has been used in previous studies (Tung et al. 2010; Zhang et al. 2024, 2022). In this study, a releasing rate of 0.20 L/min was used. The source was on for the first 5 minutes and then turned off after. In the simulations of isothermal cases, the airflow field was solved first before the source was activated. When thermal stack was present, the transient airflow field and the concentration decay were solved simultaneously. Radiation heat transfer was not activated to save computation time. The impact on the room air temperature was negligible because the temperatures of the walls, the floor, and the dummy body were all fixed.

A structured grid scheme was used. The grids in the near-floor region were refined to cope with the fast-changing velocities. The RNG k-ε model (Yakhot et al. 1992) accompanied by the logarithmic wall functions (Launder and Spalding 1974) was selected as the turbulence model because it produced validated results for the indoor environment (Srebric and Chen 2002). It also has been demonstrated to have fair accuracy in jet ventilation system (Hu et al. 2024; Wang et al. 2023). Boussinesq approximation was used to account for the buoyancy forces.

A grid independence test similar to Ref. (Huang and Gong 2024) was performed at three grid schemes (200 k, 670 k and 1350 k) and three time-step settings (80, 160 and 320 time-steps). More time steps were allocated to the first 6 minutes to capture the fast-changing flow field at the start. The vertical velocity profiles at x=0.435 m, y=1.175 m are compared in Fig. 2(a), and the temporal concentrations and airflow velocities at the point x=0.435 m, y=1.175 m, z=0.050 m are compared in Fig. 2(b). Based on the results, the final grid number of 670 k and the setting of 160-time steps (time step = 3 s for the first 6 minutes, time step = 6 s for the remaining 4 minutes) were chosen.

The commercial CFD code PHOENICS was used. Thirteen scenarios (Table 1) were simulated to explore the effects of temperature, opening mode and thermal plume on removal efficiency.

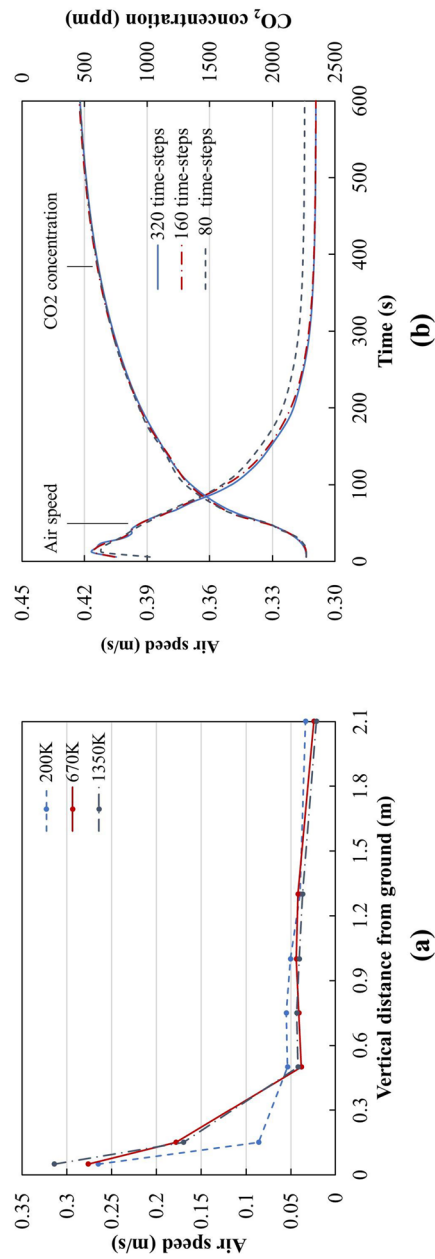


Fig. 2 Grid independence tests: **a** The grid independence test; **b** The time-step independence test

Table 1 Simulation cases (Y = On or acticated, N = Off or de-activated)

Case	Window	ΔT^a	Forced exhaust	Human thermal plume
A	N	0 °C	Y	N
B	N	0 °C	N (in the first 300 s) + Y (in the last 300 s)	N
C	Y	0 °C	Y	N
D	Y	12.5 °C	N	N
E	Y	12.5 °C	Y	N
F	Y	0 °C	Y	Y
G	N	0 °C	Y	Y
H	Y	12.5 °C	Y	Y
E1	Y	9 °C	Y	N
E2	Y	5.5 °C	Y	N
E3	Y	4 °C	Y	N
E4	Y	3 °C	Y	N
E5	Y	2 °C	Y	N

^a Temperature difference between indoor and outdoor (Only indoor temperature \geq outdoor temperature is considered)

Contaminant removal efficiency, evaluated as the ratio of the room concentration to the exhaust concentration, is commonly used to evaluate the ventilation performance in restrooms (Cetin et al. 2020; Chung and Hsu 2001; Tung et al. 2009; Zhang et al. 2022). However, it does not tell how fast a ventilation system removes the contaminants. In this study, we use the removal percentage, RP , to indicate the ventilation performance. The RP value is simply calculated as the percentage of the total released amount that has been removed within the duration of interest (10 minutes):

$$RP = \left(1 - \frac{\bar{c}_{10}V}{gt}\right) \times 100\% \quad (1)$$

where RP is the removal percentage, g is the releasing rate (g/min), t is the releasing duration ($t = 5$ minutes), \bar{c}_{10} is the average concentration in the room at the end of the 10th minute (g/m³), and V is the volume of the room (m³).

Experiments

For model validation purpose, a model restroom was constructed in accordance with Fig. 1 except that all blockages were removed. A vertical rod (cross-section: 0.047 m \times 0.047m) was positioned with five anemometers (Swema 03+; ± 0.03 m/s, ± 0.1 °C) attached as shown in Fig. 3 to measure the temperatures and airflow velocities. The distance from the sensor to the rod was 0.050 m. In addition, eight T-type thermocouples (± 0.5 °C) were deployed to measure the temperatures of walls, room air, and ambient air. The data were recorded via NI DAQ 9213. A carbon dioxide recorder was positioned in the middle of the room. All temperatures and airflow velocities were recorded every second and the CO₂ concentration was recorded every 10 seconds.

The objective was to measure the decay of CO₂ concentration in the room, which had an initial temperature of 10 °C higher than the ambient air. Before the experiment, the room was heated to the desired temperature using an electric heating mat

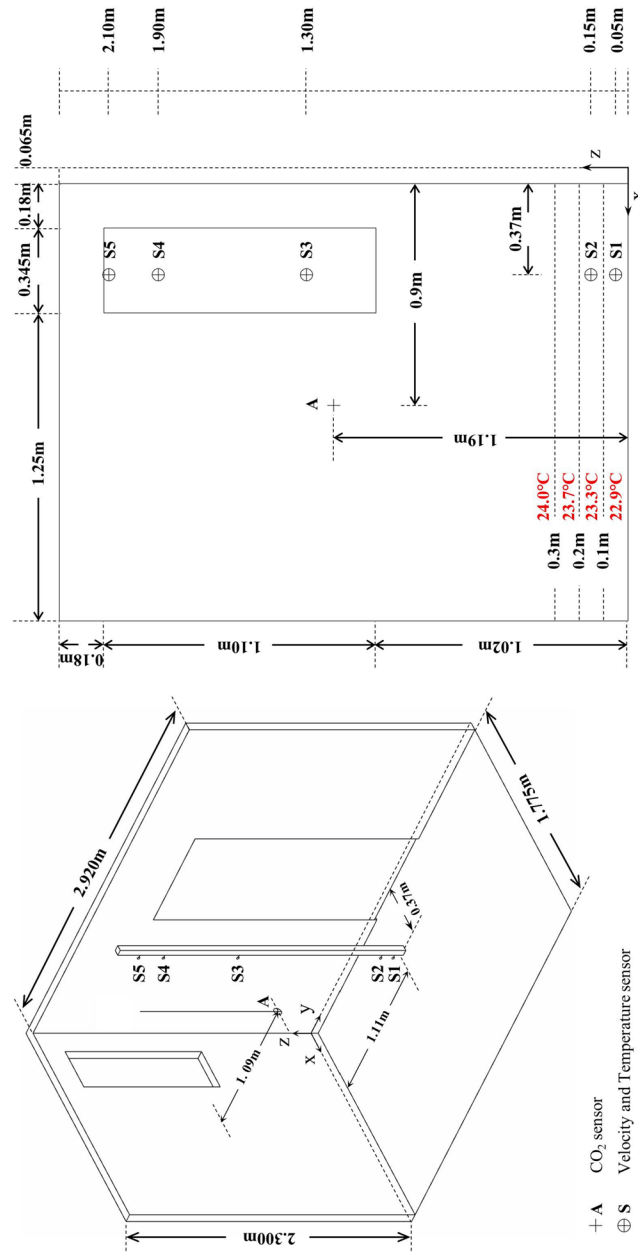


Fig. 3 A sketch of the experimental room and a section view at $y=1.16$ m

laid on the floor. The temperature was maintained for at least three hours so that a fair steady state heat transfer was established between the room and the ambient air. Then the tracer CO₂ was introduced using dry ice. A hand fan was used to stir and mix the room air to obtain a uniform distribution of CO₂. Once the CO₂ level reached above 2000 ppm, the heating mat was removed from the room. The room was then sealed using duct tape and was allowed to settle for half an hour. Then the window cover was removed. The dynamic decay started right after the window cover was removed. Except for the window, all other vents were sealed in the decay test. Previously, another decay test was conducted earlier to determine the room leakage rate of the well-sealed restroom, and the result was 0.18 h⁻¹.

The detailed settings are outlined in Fig. 3. It turned out to be difficult to achieve a uniform temperature distribution in the room. The initial temperatures at points S1 and S2 (Fig. 3), with corresponding heights of 0.05 m and 0.15 m, were 22.9°C and 23.7°C, respectively. Meanwhile, the temperatures at points S3, S4, and S5, with corresponding heights of 1.30 m, 1.90 m, and 2.10 m, were all 24.0°C.

To match the measured initial condition, the room in the CFD model was divided into four zones along the vertical direction so that a stratified temperature distribution could be set up. The detailed settings of thermal boundaries and initial concentrations are presented in Table 2.

CO₂ sensor calibration and response time determination

The CO₂ recorder (Amphenol Telaire T6713, ±30 ppm ± 3% of reading) was calibrated against a commercial standard CO₂ gas (4020 ppm) and the background concentration of atmospheric CO₂ (the average monthly CO₂ level in May 2023 is 424ppm (Ian Tiseo 2024)).

It was found later that the measured concentration lagged the simulated concentration. Therefore, the response time of the CO₂ sensor was determined. A calibration procedure was setup as shown in Fig. 4. First the chamber (54 L) was charged with CO₂ flow to reach a high concentration. The CO₂ sensor was placed in the chamber. A fan was also placed inside the chamber to mix the air. Then clean airflow was introduced into the chamber at a constant flow rate (Seven Star D07-19F, ±1 % F.S.). For a well-mixing condition, the concentration decay inside the chamber can be well predicted. By comparing the theoretical CO₂ decay curve with the measured one, the response time was then obtained. Three tests were performed with their results shown in Table 3 and Fig. 5. Finally, an average response time (t₀=57.7 s) was then obtained for the sensor.

Table 2 Wall boundary conditions and initial concentrations

	E Wall	S Wall	W Wall (Window)	N Wall (Door)	Ceiling	Floor	Room	Outside
Temperature (°C)	23.6	23.7	22.8	23.1	23.1	21.6	Fig. 3	11.2
Concentration (ppm)	-	-	-	-	-	-	2291	424

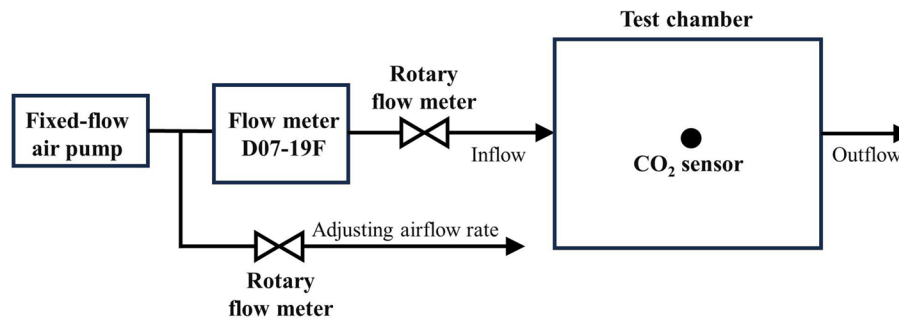


Fig. 4 Experimental configuration for the determination of CO₂ sensor response time

Table 3 Experimental parameters and the resulting values of response time

Group	Flow Rate (L/s)	Ambient CO ₂ Concentration (ppm)	Initial Concentration (ppm)	Response Time (s)	Average Response Time t_0 (s)
A	0.182	426	2855	45	57.7s
B	0.146	424	2486	62	
C	0.107	433	1602	66	

Result and discussion

Validation result

The measured concentration at point A (Fig. 3), adjusted by response time $t_0 = 57.7$ s is compared with the CFD predictions in Fig. 6. The agreement is good in general. This suggests that the CFD model predicts the CO₂ decay with reasonable accuracy.

Airflow velocities and temperatures measured along the rod are compared with the simulation for the 30th, 120th, 330th, and 600th seconds in Fig. 7. The general trends are predicted although a noticeable difference in velocity is observed at point S2 (H=0.15m). In the simulation, the cold incoming airflow is more confined to the proximity of the floor while the measured flow was thicker, resulting in higher temperatures and velocities at point H=0.15 m. This indicates that the incoming cold flow acted more like a jet, which could not be modeled well by the RNG k- ϵ model.

The temporal variations of velocities and temperatures are also presented in Fig. 7 for the lower three points. The discrepancy between the experiment and simulation is noticeable at point H=0.15 m. Close to the floor, the maximum airflow velocity reaches 0.5 m/s. Both simulation and experiment show that the flow velocity slows down as the room temperature drops. This is predictable because the driving force weakens as the difference between indoor and outdoor temperature decreases.

The reason for the discrepancy between the measured and simulated airflow velocities and temperatures at H=0.15 m is further explored. The contour plots of the airflow velocity at section $x=0.435$ m six seconds after the opening of the window are shown in Fig. 8. The cold jet is clearly visible as it drops down to the floor from the window and then moves forward on the floor surface. S2 (H=0.15 m) is at the upper edge of the jet, where the velocity changes rapidly, making it difficult for the model to capture. The velocity is particularly sensitive to the location in the z-axis direction.

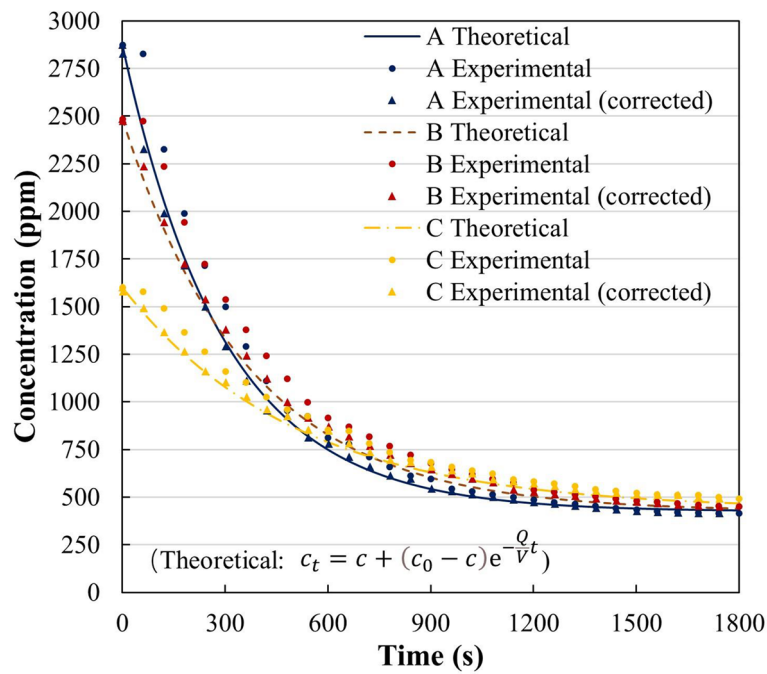


Figure 5 Decay curves of concentrations over time

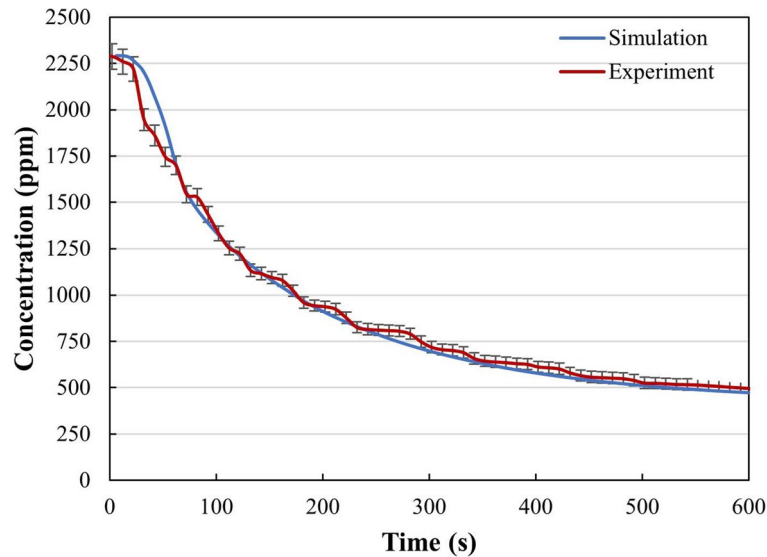


Fig. 6 Decay curves of concentrations over time

As shown in Fig. 9, the simulated velocity at S6 ($H=0.10\text{m}$) is closer to the measured velocity at S2 ($H=0.15\text{m}$) than the simulated velocity at S2, which suggests that the jet thickness is under-predicted. Furthermore, the initial room air in the CFD simulation is assumed to be still while in the experiment it was most likely not still because a uniform temperature field was difficult to establish. The electric heating mat had left a warm spot at the floor surface after it was extracted. And this warm spot might not have faded away completely at the start of the measurement. These differences

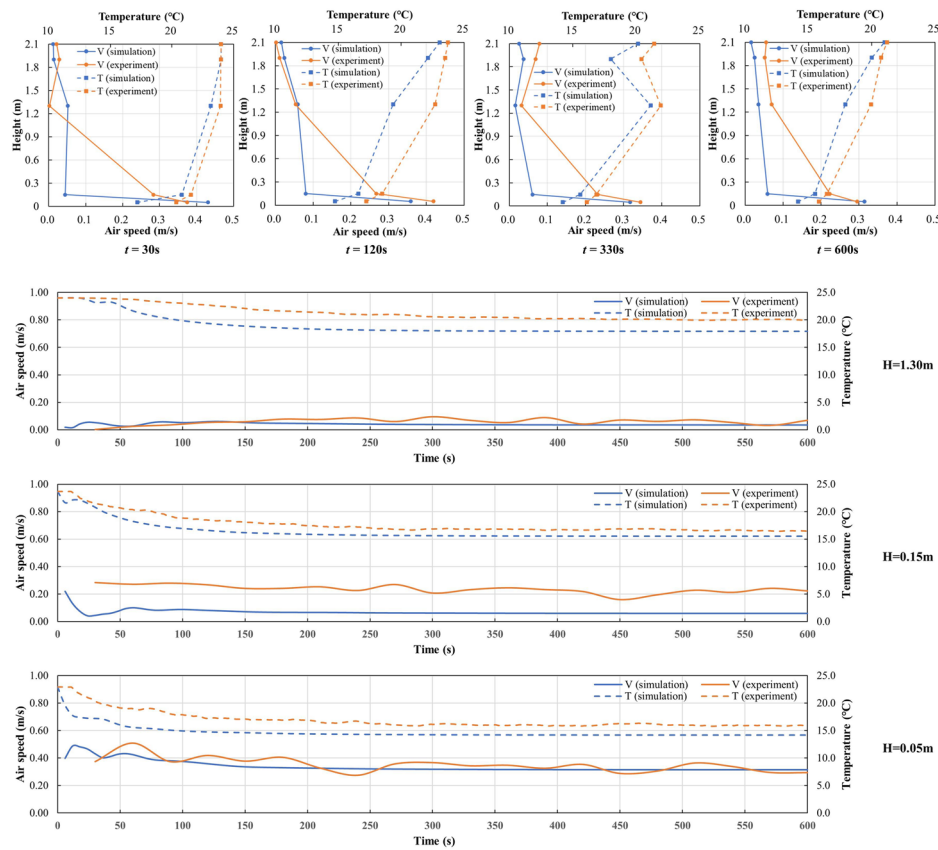


Fig. 7 Airflow velocity and temperature variations over time

and uncertainties may contribute to the discrepancy between the simulation and the measurement.

Despite disparities in temperature and velocity between the measurements and the simulation, the CFD model predicted the trends of temperature and velocity. Especially, the concentrations of carbon dioxide were well predicted. Therefore, the CFD model is considered reliable for simulating carbon dioxide concentrations. In future studies, a perhaps more detailed and effective validation can be done with the help of a more powerful velocity measurement tool-particle image velocimetry, as demonstrated by Szczepanik-Scislo et al. (Szczepanik-Scislo et al. 2019).

Comparisons of removal percentage

Figure 10 presents a summary of the simulation results for eight of the cases. The values of the removal percentage by Equation (1) are shown in Fig. 10(a). Figure 10(b) summarizes the three fates of the release pollutants (totally 2.13g): discharged amount by the fan, discharged amount by the window, and those remained in the room. The accumulated errors in mass balances from all time steps are no more than 3.2%.

Case A represents a normal operation of the restroom with mechanical ventilation only. The exhaust fan provides an ACH of 10 h⁻¹. The removal percentage at $t = 10$ min

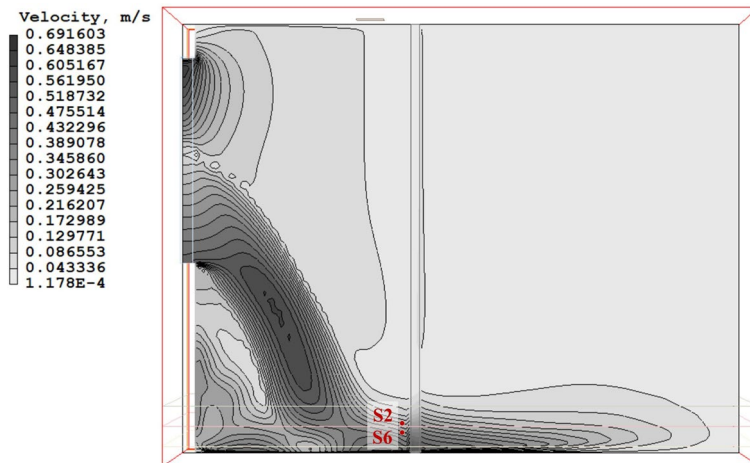


Fig. 8 Simulated velocity contour at $t = 6$ s

is $RP = 68.5\%$, which suggests that approximately one third of the pollutant still remains in the room 5 minutes after the release ceases.

Case C is same as Case A except that the window is open as an additional inlet in addition to the door seam and vents. The removal percentage drops to only 49.6%, indicating that opening the window does not help remove the pollutant in the absence of thermal draft. The reason for decreased efficiency can be seen in Fig. 11, which shows the streamlines of the fresh air from the window. The upper part of the fresh air is directly discharged by the exhaust fan without passing through the location of the source. This short-circuit of fresh air reduces the effective ventilation rate in Case C compared with Case A although both cases have the same ventilation rate.

Delaying the activation of the exhaust fan will reduce the removal percentage as demonstrated in Case B, where the exhaust fan is turned on at $t = 300$ s, right after the release stops. The removal percentage $RP = 42.6\%$ is the lowest among the eight cases.

The removal percentages in cases D, E, and H all exceed 97%, suggesting that window-induced stack ventilation can effectively enhance the pollutant removal. The thermal plume generated by the human body also have positive effects especially when stack ventilation is absent. The presence of the human thermal plume increases the removal percentage by 14.3% when the window is closed (case G vs. case A) and by 27.5% when

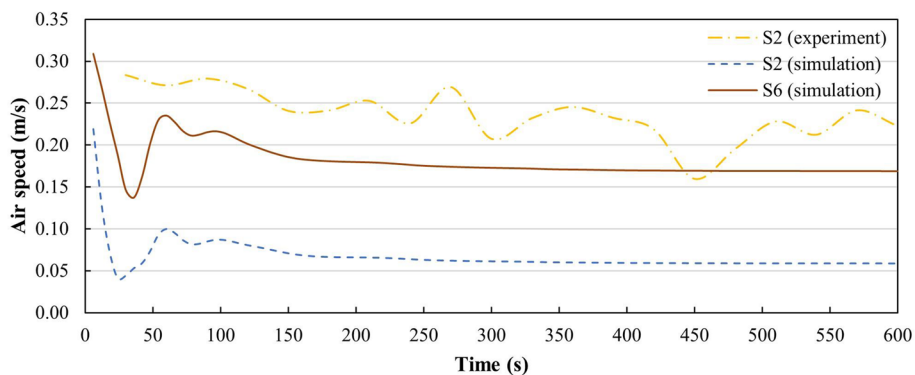


Fig. 9 Influence of point positions on airflow velocity

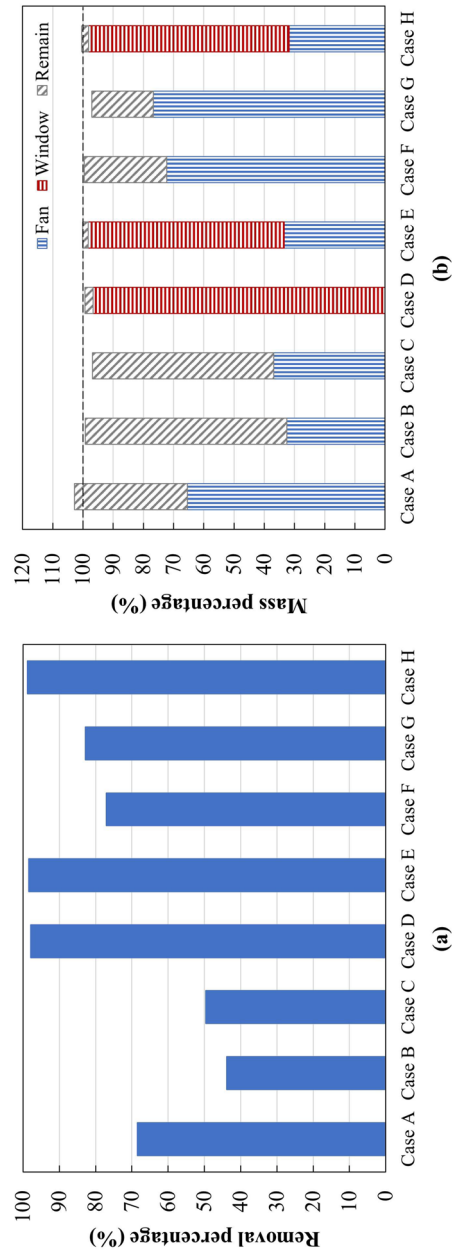


Fig. 10 Simulation results: **a** Removal percentage; **b** Accumulated mass balances of pollutant mass

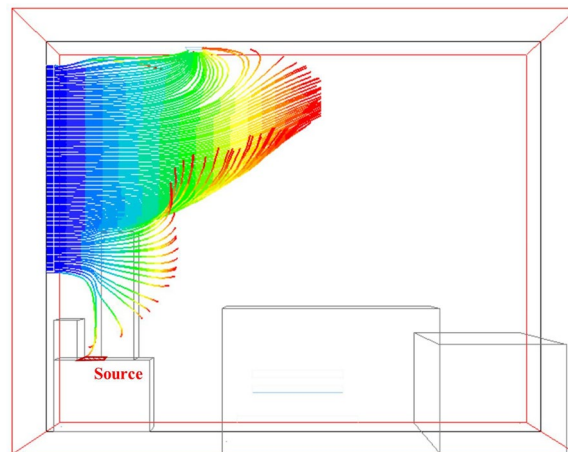


Fig. 11 Air streamlines at plan $y=1.3\text{m}$ in Case C at $t = 30\text{s}$

the window is open (case F vs. case C). However, the effect of the human thermal plume on the removal percentage is negligible when there is strong stack effect at the window (case E vs. case H).

Discussion on the impact of stack effect

The impact of stack effect is further explored in this section. Two temperature differences contribute to the stack effect in the restroom. One is the stack effect due to difference between indoor and outdoor temperatures. The other is the human thermal plume.

Stack ventilation can be very effective in removing the pollutants. At a temperature difference of $\Delta t = 12.5^\circ\text{C}$ between the indoor and the outdoor, case E has the highest removal percentage of 98.4%, increased by more than 43.6% ($= (98.4\% - 68.5\%) / 68.5\%$) from that of the base case (case A, 68.5%). The reasons can be seen in Fig. 12, which shows the velocity vectors at a section cut through the window in case A and case E. Two differences can be identified. Firstly, case E has a more favorable flow pattern for the pollutant removal. The cold air from the window flows into the room and drops towards the source, effectively participating in the dilution of pollutants. The dropping flow effectively lifts and expels the polluted air from the occupied zone towards the exhaust fan and the upper section of the window. Secondly, the window generates its own ventilation. The stack ventilation rate is highest at the beginning and then decreases as more cold air flows into the room and reduces the difference between indoor and outdoor temperatures. The total ventilation rate under this hybrid ventilation scheme decreases from the initial value of 34 h^{-1} and gradually levels off and reaches 29 h^{-1} at the end of the 10th minute. The 10-min average ventilation rate is about 30 h^{-1} , almost 3 times of that under solely exhaust ventilation. The increase in ventilation rate leads to a higher removal percentage. If the removal efficiency is used as the indicator, the conclusion would be different as this indicator only concerns with the ratio of the room concentration to the exhaust concentration, both decreasing over time. As shown by Tung et al. (Tung et al. 2009) in their measurements, the removal efficiency hardly changed as the ventilation rates increased from 8.5 h^{-1} to 17 h^{-1} . Instead, our study shows that the removal percentage is associated with the ventilation rate, which conforms to the common sense that

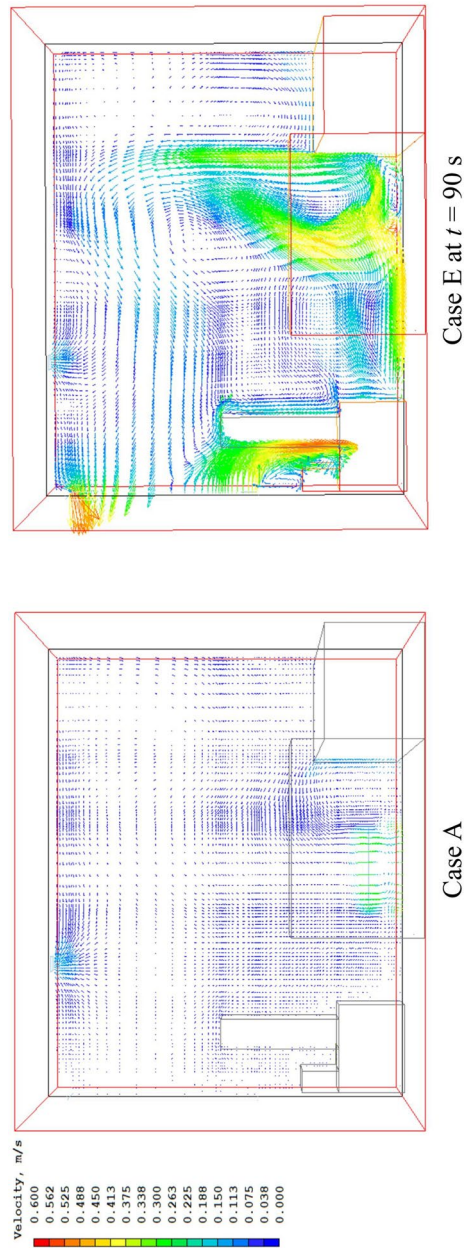


Fig. 12 Airflow velocity distributions at $y=1.435$ m of Case A (all time) and Case E (at $t = 90$ s)

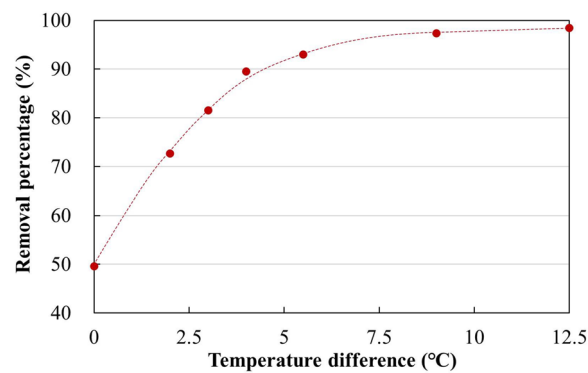


Fig. 13 Relationship between removal percentage and temperature difference

ventilation rates have a considerable impact on indoor IAQ (Aganovic et al. 2021; Wargocki et al. 2002).

The benefits of window-induced ventilation can be minimized by the possible short-circuit when the stack effect is weak. Therefore, the effect of different temperature differences is further investigated as shown in Fig. 13. At a zero-temperature difference, the removal percentage drops to below 50% from 68.5% (Case A) due to adverse short circuit effect. As the temperature difference increases, the removal percentage increases rapidly and returns back to 68.5% at approximately $\Delta t = 1.6^\circ\text{C}$. The percentage reaches above 93% at $\Delta t = 5.5^\circ\text{C}$ and then starts to level off after. At $\Delta t = 12.5^\circ\text{C}$, the removal percentage reaches above 98%.

Unlike the thermal stack at the window, the human thermal plume does not introduce additional ventilation and has weaker influence. Its apparent effect depends on the presence of stack ventilation. The human thermal plume has notable effect on the removal percentage when stack ventilation is absent at the window. When other factors are all equal, case G (with human thermal plume, 82.9%) is more efficient than case A (68.5%), and case F (with human thermal plume, 77.1%) is more efficient than case C (49.6%). However, when the window associated stack effect is present, the effect of the human plume is negligible. Case E (98.4%) and case H (98.8%) have similar values of the removal percentage. Fig. 14 compares the vector plots between case F (window closed) and case H (window open for stack ventilation). The human thermal plume favors the removal of the pollutant with the source located right behind the thermal plume in case F while this plume is suppressed by the buoyancy flow from the window in case H. Note that case E (without human plume) has a slightly higher removal percentage than case H (with human plume), indicating that the presence of human thermal plume can weaken the effect of the buoyancy flow from the window. This highlights the importance of plume locations when multiple thermal plumes are present as they will interact with each. Such interaction can cause negative effect on the removal percentage.

Discussion on pollutant exposure

Exposure assessment is another method to evaluate ventilation efficiency. Exposure levels at two locations are calculated. The first location is the at breathing spot (height: 1.4 m) of the sitting dummy. This exposure reflects the current user's risk. The second location is at the breathing level of the whole room. This exposure reflects the risk of the next

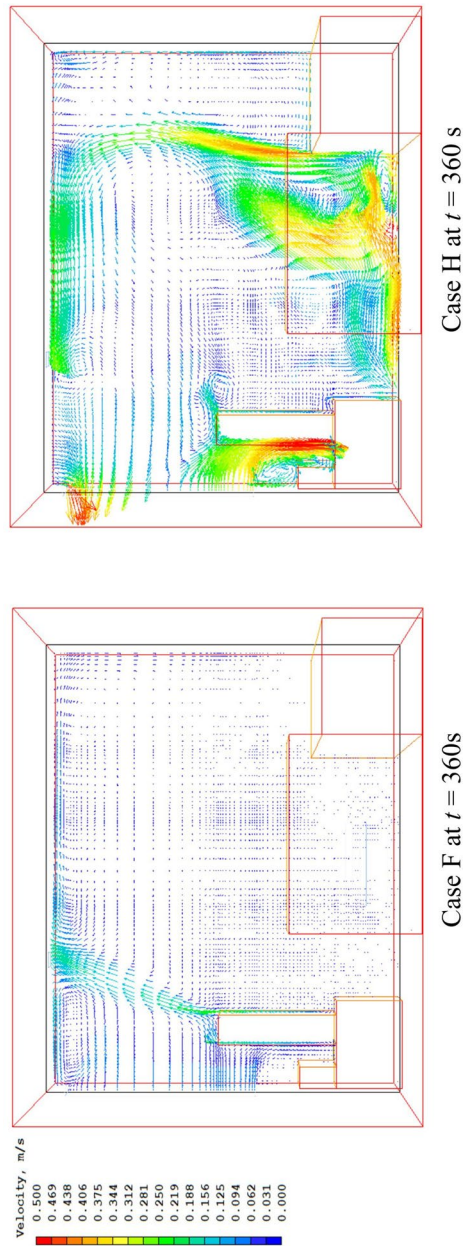


Fig. 14 Airflow velocity distributions at $y=1.435m$ of Case F and Case H (at $t = 360s$)

immediate user, who could be anywhere in the room. When the previous user leaves the room, the washing and walking actions will disturb the airflow and the concentration distribution, the modeling of which is beyond the scope of this study. For simplicity, the exposure is assessed without the consideration of this disturbance.

It is assumed that the preceding user spends 5 minutes in a sitting position and the subsequent user stays in the restroom for the next 5 minutes in a standing position. The average concentration for the first 5 minutes at the first location is referred to as the exposure of the current user. The exposure of the standing user is evaluated at three heights: 1.5 m, 1.6 m, and 1.7 m. The concentrations at each level are averaged for the next 5 minutes to represent the exposure of the next user. The calculated results are shown in Fig. 15. It turns out that the exposure of the standing user is not sensitive to the breathing height. The pollutant in case B does not disperse to the breathing zone in the first 5 minutes in an absolutely still room, but this situation is rare in real life.

Case A represents a base case with the window closed and the absence of human thermal plume. Case G represents the base case with the window closed and the presence of human thermal plume. When there is no stack effect, opening the window can reduce the pollutant exposure for both the current and the subsequent user (case C vs case A). This applies in a hot summer day when the ambient and body temperatures are very close. In reality, however, the presence of thermal plume is more common. With the consideration of the human thermal plume, opening the window reduces the pollutant exposure for the current user but will make the subsequent user inhale more pollutants (case F vs. case G). When there is stack ventilation, the result is slightly different. Regardless of whether the impact of the human thermal plume is considered, opening the window will make the current user inhale more pollutants but will significantly decrease the pollutant exposure of the subsequent user (case E vs. case A, case H vs. case G). In other words, for the current user, opening the window is favorable when it is not colder outside but becomes unfavorable when it is colder outside. For the subsequent user, opening the window is favorable when it is colder outside but can become unfavorable when it is not colder outside. Further analyses show that the subsequent standing user's exposure change is more associated with the removal percentage because the evaluation is conducted using an area-averaged concentration. In comparison, the sitting person is evaluated at one particular spot. The concentration is more site specific and depends not only on the removal percentage but also on other factors such as vicinity to the inlet, airflow direction, etc. For example, the concentration at the sitting position is strongly affected by the dilution of fresh air from the window and at the same time, by the interaction of the window associated buoyancy flow and the human thermal plume.

Discussion on indoor thermal comfort and surface resuspension

The previous analyses have demonstrated that window-induced cold draft can increase ventilation rates substantially. This cold fresh air can cause dissatisfied thermal comfort to users in winter. To examine the impact of window associated thermal draft on the occupant's thermal comfort, the Predicted Mean Vote (PMV) are evaluated at two locations in case G (exhaust ventilation with human plume but no window) and case H (exhaust ventilation with human plume and window draft at $\Delta t = 12.5^\circ\text{C}$). The first location is at the top of the head of the sitting dummy. The second location is at the

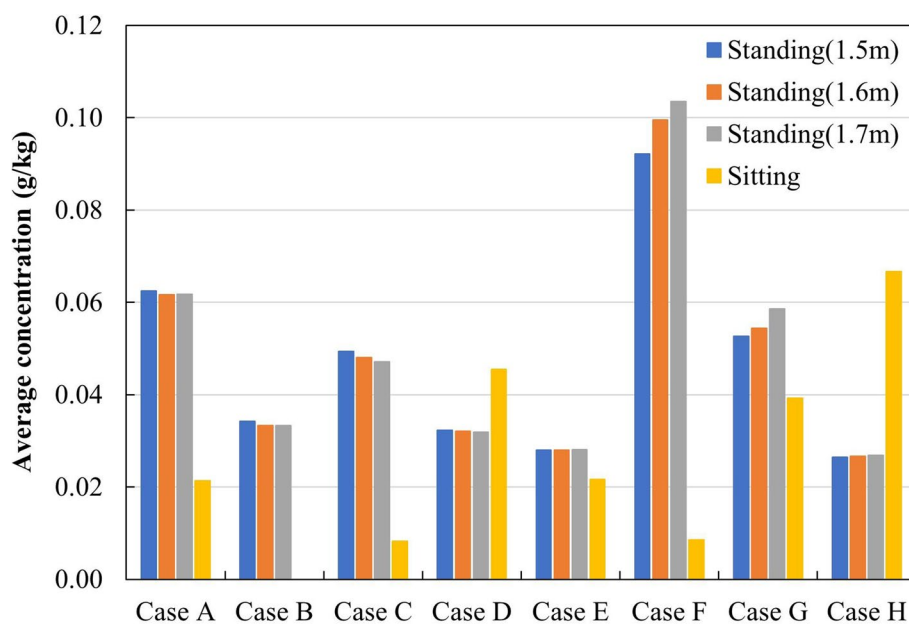


Fig. 15 Average concentration of breathing zone at of different cases

breathing level of a possible immediate next user, standing before the sink. The coordinates of these two locations and other input parameters are given in Table 4. The determination of relative humidity can be complicated. Although the outdoor air is colder and drier, its relative humidity could be higher. It is possible to determine the distribution of relative humidity in simulation with given boundary conditions. However, the modeling itself would be out of the scope of this study. For simplicity, the PMV is estimated for a range of relative humidity (30% to 60%) using the Center for the Built Environment Thermal Comfort Tool, which complies with ASHRAE 55–2017, ISO 7730:2005 and EN 16798–1:2019 Standards (Tartarini et al. 2020). The results are shown in Fig. 16.

With mechanical ventilation only (case G), the PMV values at both locations consistently remain within the thermal comfort range of -0.5 to 0.5. When stack ventilation is introduced (case H), the PMV values at both locations decrease considerably and fall outside the thermal comfort zone ($PMV < -0.5$). For the sitting user, the PMV values drop to below -1.0 shortly after opening the window. The influence of relative humidity on PMV values appears to be limited. The reduction in temperature and the increase in airflow velocity are the major drivers for the decrease of thermal comfort. Changes in temperature and velocity are minimal in case G with exhaust ventilation only. In contrast, in case H, the airflow velocity increases considerably in addition to a cold draft of $\Delta t = 12.5^\circ\text{C}$. Fig. 17 shows the maximum airflow velocities at three surfaces: the floor, the top of the toilet, and the sink. These surface airflow velocities can reach above 0.7 m/s, exceeding the recommended range, typically 0.2 m/s to 0.3 m/s, for indoor air.

The higher airflow velocity also increases particle resuspension from the surfaces (Boor et al. 2013; Henry 2016; Henry and Minier 2014; Zhang et al. 2018). According to Liu et al. (Liu et al. 2020), the particle resuspension rate increases almost linearly with the increase of the airflow velocity. When the airflow velocity increases from 0.2 m/s to 0.7 m/s, the risk of resuspension increases by approximately five times. With the evidence of

Table 4 Details of PMV evaluation point

Coordinate	X(m)	Y(m)	Z(m)	Clothing level(clo)	Metabolic rate(met)
Sitting	0.35	1.425	0.85	1 (typical winter indoor clothing)	1.0 (seated, quiet)
Standing	1.75	0.85	1.0		1.2 (standing, relaxed)

the presence of bacteria, viruses, and other pollutants on various surfaces in restrooms (Dancer et al. 2021; Ding et al. 2020; Hu et al. 2020; Ma et al. 2021), the health risk associated with the pathogen resuspension by window-induced stack ventilation cannot be neglected.

In summary, although stack ventilation can increase the removal percentage considerably, the side effect includes reduced thermal comfort and increased risks associated with strengthened particle resuspension. Our analyses are far from completed and comprehensive but highlight the importance of further studies on this topic.

Conclusions

In this study, the ventilation performance in residential restroom spaces is revisited with a focus on short-term contaminant removal rate in response to window opening. We propose to use the removal percentage in evaluating the contaminant removal performance of restroom ventilation instead of using the conventional indicator -- removal efficiency. With results obtained through CFD simulations, we use this indicator to quantitatively evaluate the effects of window opening, exhaust fan use, indoor and outdoor temperature difference, and occupant thermal plume on the performance of restroom ventilation in removing instantly released contaminants. The following conclusions can be drawn.

- The short-term pollutant removal performance of mechanical ventilation is limited. The 10-min removal percentage under exhaust ventilation at an ACH of 10 h^{-1} is 68.5%. Opening the window causes short-circuit of fresh air and reduces the pollutant removal percentage to 49.6%. When the indoor and outdoor temperature difference is less than $2 \text{ }^\circ\text{C}$, window should be kept closed under exhaust ventilation.
- Window-induced stack ventilation can greatly increase the removal percentage by increasing the ventilation rate and by improving the airflow pattern. The removal percentage increases as the temperature difference increases. A removal percentage of over 98% is achieved at a temperature difference of $12.5 \text{ }^\circ\text{C}$.
- The human thermal plume has notable effect on the removal percentage, but its effect on the removal percentage can be neglected in the presence of stack ventilation at the window.
- In winter, opening the window may increase the pollutant exposure to pollutants generated during the toilet use for the current sitting user but can reduce the exposure for the next standing user. In addition, the current user may experience an increased cold airflow velocity and reduced thermal comfort. The maximum indoor airflow velocity can reach 0.6 m/s to 0.7 m/s . The predicted mean vote can drop to $\text{PMV} = -0.9 \sim -1.3$.

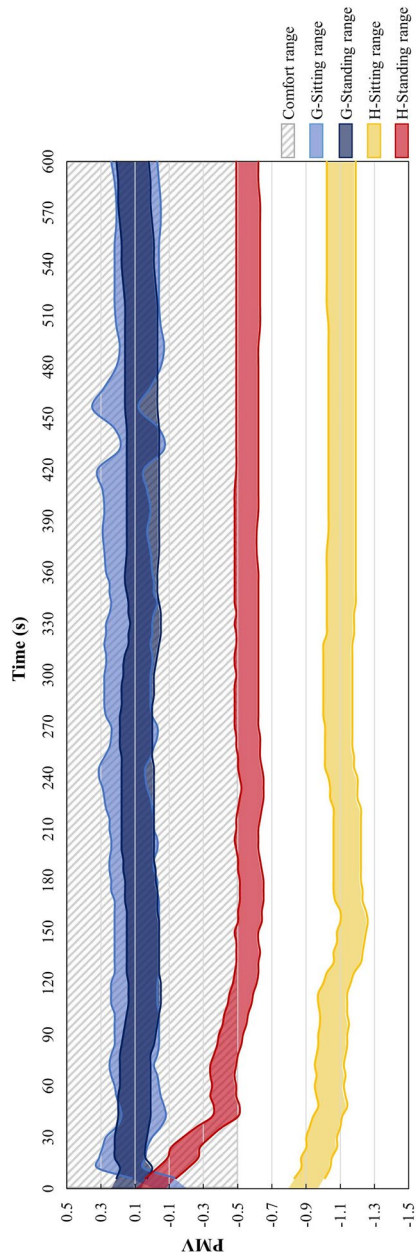


Fig. 16 Estimated PMV ranges at two locations in case G and case H

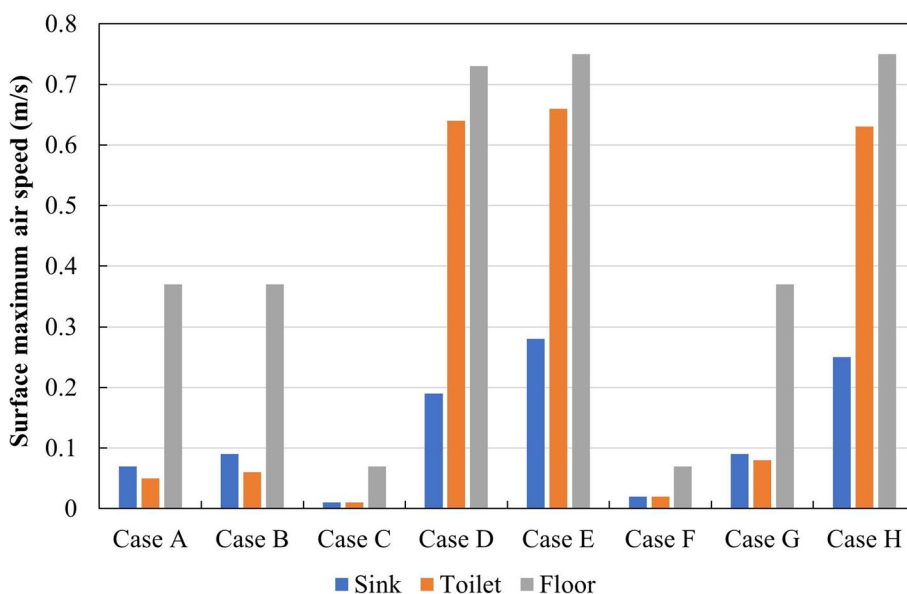


Fig. 17 Maximum airflow velocities 0.01m above the selected surfaces

- In CO₂ decay tests for CFD validation purposes, the response time of the sensor should be checked and calibrated if necessary.

The addition of buoyancy-driven ventilation to exhaust ventilation in a restroom by opening the window can increase the short-term removal percentage considerably although the adverse effects include dropped thermal comfort, increased exposure on the current sitting user, and risks associated with strengthened particle resuspension. Our study highlights the importance of further studies on the short-term evaluation of the removal percentage of restrooms.

Authors' contributions

Yuyao Chen: Data curation, Formal analysis, Writing-Original draft preparation; Zhiqiang Zhai: Reviewing, Supervision; Yuan Zhe: Data curation; Guoqing He: Conceptualization, Methodology, Supervision, Writing and Editing, Funding acquisition.

Funding

This work was supported by Zhejiang Provincial Natural Science Foundation of China (Grant No LY21E080023).

Availability of data and materials

Data sharing is not applicable to this article as no datasets were generated or analysed during the current study.

Declarations

Ethics approval and consent to participate

Ethics approval was not required for this research.

Competing interests

The authors declare that they have no known competing financial interests or personal relationships that could have appeared to influence the work reported in this paper.

Received: 13 March 2024 Accepted: 2 June 2024

Published online: 21 June 2024

References

- Aganovic A, Bi Y, Cao G, Drangsholt F, Kurnitski J, Wargocki P (2021) Estimating the impact of indoor relative humidity on SARS-CoV-2 airborne transmission risk using a new modification of the Wells-Riley model. *Build. Environ.* 205:108278. <https://doi.org/10.1016/j.buildenv.2021.108278>
- Ai Z, Mak CM, Gao N, Niu J (2020) Tracer gas is a suitable surrogate of exhaled droplet nuclei for studying airborne transmission in the built environment. *Build. Simul.* 13:489–496. <https://doi.org/10.1007/s12273-020-0614-5>
- Ali W, An D, Yang Y, Cui B, Ma J, Zhu H, Li M, Ai X-J, Yan C (2022) Comparing bioaerosol emission after flushing in squat and bidet toilets: Quantitative microbial risk assessment for defecation and hand washing postures. *Build. Environ.* 221:109284. <https://doi.org/10.1016/j.buildenv.2022.109284>
- Ameen A, Cehlin M, Larsson U, Karimipannah T (2019) Experimental investigation of ventilation performance of different air distribution systems in an office environment—heating mode. *Energies* 12:1835. <https://doi.org/10.3390/en12101835>
- ASHRAE (2019) Ventilation for Acceptable Indoor Air Quality. ANSI/ASHRAE Standard 62.1-2019. Atlanta, GA, USA
- Barker J, Jones MV (2005) The potential spread of infection caused by aerosol contamination of surfaces after flushing a domestic toilet. *J. Appl. Microbiol.* 99:339–347. <https://doi.org/10.1111/j.1365-2672.2005.02610.x>
- Boor BE, Siegel JA, Novoselac A (2013) Monolayer and multilayer particle deposits on hard surfaces: literature review and implications for particle resuspension in the indoor environment. *Aerosol Sci Technol* 47:831–847. <https://doi.org/10.1080/02786826.2013.794928>
- Cai J, Sun W, Huang J, Gamber M, Wu J, He G (2020) Indirect virus transmission in cluster of COVID-19 cases, Wenzhou, China, 2020. *Emerg Infect Dis* 26:1343–1345. <https://doi.org/10.3201/eid2606.200412>
- Cao X, Hao G, Li Y, Wang M, Wang J-X (2022) On male urination and related environmental disease transmission in restrooms: From the perspectives of fluid dynamics. *Sustain. Cities Soc.* 80:103753. <https://doi.org/10.1016/j.scs.2022.103753>
- Cetin YE, Avci M, Aydin O (2020) Influence of ventilation strategies on dispersion and removal of fine particles: An experimental and simulation study. *Sci. Technol. Built Environ.* 26:349–365. <https://doi.org/10.1080/23744731.2019.1701332>
- Chen Y, Chen L, Deng Q, Zhang G, Wu K, Ni L, Yang Y, Liu B, Wang W, Wei C, Yang J, Ye G, Cheng Z (2020) The presence of SARS-CoV-2 RNA in the feces of COVID-19 patients. *J. Med. Virol.* 92:833–840. <https://doi.org/10.1002/jmv.25825>
- Cheng Z, Guangyu C, Aganovic A, Baizhan L (2020) Experimental study of the interaction between thermal plumes and human breathing in an undisturbed indoor environment. *Energy Build.* 207:109587. <https://doi.org/10.1016/j.enbuid.2019.109587>
- Chung KC, Hsu SP (2001) Effect of ventilation pattern on room air and contaminant distribution. *Build Environ* 36(9):989–998. [https://doi.org/10.1016/S0360-1323\(00\)00051-2](https://doi.org/10.1016/S0360-1323(00)00051-2)
- Dancer SJ, Li Y, Hart A, Tang JW, Jones DL (2021) What is the risk of acquiring SARS-CoV-2 from the use of public toilets? *Sci. Total Environ.* 792:148341. <https://doi.org/10.1016/j.scitotenv.2021.148341>
- Ding Z, Qian H, Xu B, Huang Y, Miao T, Yen H-L, Xiao S, Cui L, Wu X, Shao W, Song Y, Sha L, Zhou L, Xu Y, Zhu B, Li Y (2020) Toilets dominate environmental detection of SARS-CoV-2 virus in a hospital (preprint). *Infectious Diseases (except HIV/AIDS)*. <https://doi.org/10.1101/2020.04.03.20052175>
- Fisk WJ, Faulkner D, Sullivan D, Bauman F (1997) Air change effectiveness and pollutant removal efficiency during adverse mixing conditions. *Indoor Air* 7:55–63. <https://doi.org/10.1111/j.1600-0668.1997.t01-3-00007.x>
- Gerba CP, Wallis C, Melnick JL (1975) Microbiological hazards of household toilets: droplet production and the fate of residual organisms. *Appl Microbiol* 30(2):229–237. <https://doi.org/10.1128/am.30.2.229-237.1975>
- He G, Yang X, Srebric J (2005) Removal of contaminants released from room surfaces by displacement and mixing ventilation: modeling and validation. *Indoor Air* 15:367–380. <https://doi.org/10.1111/j.1600-0668.2005.00383.x>
- Tiseo I (2024) Average monthly carbon dioxide (CO₂) levels in the atmosphere worldwide from 1990 to 2023. *statista*. <https://www.statista.com/statistics/1091999/atmospheric-concentration-of-co2-historic/>
- Henry C, Minier J-P (2014) Progress in particle resuspension from rough surfaces by turbulent flows. *Prog. Energy Combust. Sci.* 45:1–53. <https://doi.org/10.1016/j.pecs.2014.06.001>
- Henry C (2016) Surface forces and their application to particle deposition and resuspension. part. wall-bounded turbul. *Flows Depos. Re-Suspens. Agglom.* volume 571. https://doi.org/10.1007/978-3-319-41567-3_5
- Hu X, Xing Y, Ni W, Zhang F, Lu S, Wang Z, Gao R, Jiang F (2020) Environmental contamination by SARS-CoV-2 of an imported case during incubation period. *Sci. Total Environ.* 742:140620. <https://doi.org/10.1016/j.scitotenv.2020.140620>
- Hu J, Kang Y, Lu Y, Yu J, Zhong K (2024) A simple method and prediction model for calculating the cooling load of impinging jet ventilation system in office buildings. *Build. Environ.* 254:111408. <https://doi.org/10.1016/j.buildenv.2024.111408>
- Huang Y, Gong G (2024) Transient simulation and experimental analysis for the response of dual-cycle air-carrying energy radiant diffuse terminal. *J. Clean. Prod.* 451:142094. <https://doi.org/10.1016/j.jclepro.2024.142094>
- Hwang SE, Chang JH, Oh B, Heo J (2021) Possible aerosol transmission of COVID-19 associated with an outbreak in an apartment in Seoul, South Korea, 2020. *Int. J. Infect. Dis.* 104:73–76. <https://doi.org/10.1016/j.ijid.2020.12.035>
- Johnson D, Lynch R, Marshall C, Mead K, Hirst D (2013) Aerosol generation by modern flush toilets. *Aerosol Sci Technol* 47:1047–1057. <https://doi.org/10.1080/02786826.2013.814911>
- Kang M, Wei J, Yuan J, Guo J, Zhang Y, Hang J, Qu Y, Qian H, Zhuang Y, Chen X, Peng X, Shi T, Wang J, Wu J, Song T, He J, Li Y, Zhong N (2020) Probable evidence of fecal aerosol transmission of SARS-CoV-2 in a high-rise building. *Ann Intern Med.* <https://doi.org/10.7326/M20-0928>
- Launder BE, Spalding DB (1974) The numerical computation of turbulent flows. *Comput. Methods Appl. Mech. Eng.* 3:269–289. [https://doi.org/10.1016/0045-7825\(74\)90029-2](https://doi.org/10.1016/0045-7825(74)90029-2)

- Lee MCJ, Tham KW (2021) Public toilets with insufficient ventilation present high cross infection risk. *Sci. Rep.* 11:20623. <https://doi.org/10.1038/s41598-021-00166-0>
- Lin Y-P (2021) Natural ventilation of toilet units in K–12 school restrooms using CFD. *Energies* 14:4792. <https://doi.org/10.3390/en14164792>
- Liu Z, Niu H, Rong R, Cao G, He B-J, Deng Q (2020) An experiment and numerical study of resuspension of fungal spore particles from HVAC ducts. *Sci. Total Environ.* 708:134742. <https://doi.org/10.1016/j.scitotenv.2019.134742>
- Liu Z, Yin D, Niu Y, Cao G, Liu H, Wang L (2022) Effect of human thermal plume and ventilation interaction on bacteria-carrying particles diffusion in operating room microenvironment. *Energy Build.* 254:111573. <https://doi.org/10.1016/j.enbuild.2021.111573>
- Liu Z, Wang T, Wang Y, Liu H, Cao G, Tang S (2023) The influence of air supply inlet location on the spatial-temporal distribution of bioaerosol in isolation ward under three mixed ventilation modes. *Energy Built Environ.* 4:445–457. <https://doi.org/10.1016/j.enbenv.2022.03.002>
- Luo D, Huang J, Zheng X, Liu F, Li Y, Wang Y, Qian H (2023) Spread of flushing-generated fecal aerosols in a squat toilet cubicle: Implication for infection risk. *Sci. Total Environ.* 859:160212. <https://doi.org/10.1016/j.scitotenv.2022.160212>
- Ma J, Qi X, Chen H, Li X, Zhang Z, Wang H, Sun L, Zhang L, Guo J, Morawska L, Grinshpun SA, Biswas P, Flagan RC, Yao M (2021) Coronavirus disease 2019 patients in earlier stages exhaled millions of severe acute respiratory syndrome coronavirus 2 per hour. *Clin Infect Dis* 72:e652–e654. <https://doi.org/10.1093/cid/ciaa1283>
- Ministry of Housing and Urban-Rural Development (2012) Design code for heating ventilation and air conditioning of civil buildings. China Architecture & Building Press, Beijing, China
- Mui K, Wong L, Yu H, Cheung C, Li N (2017) Exhaust ventilation performance in residential washrooms for bioaerosol particle removal after water closet flushing. *Build. Serv. Eng. Res. Technol.* 38:32–46. <https://doi.org/10.1177/0143624416660597>
- Rim D, Novoselac A (2010) Ventilation effectiveness as an indicator of occupant exposure to particles from indoor sources. *Build. Environ.* 45:1214–1224. <https://doi.org/10.1016/j.buildenv.2009.11.004>
- Rueda López MJ, Guyot G, Golly B, Ondarts M, Wurtz F, Gonze E (2021) Relevance of CO₂-based IAQ indicators: Feedback from long-term monitoring of three nearly zero-energy houses. *J. Build. Eng.* 44:103350. <https://doi.org/10.1016/j.jobe.2021.103350>
- Sato H, Morimatsu H, Kimura T, Moriyama Y, Yamashita T, Nakashima Y (2002) Analysis of malodorous substances of human feces. *J Health Sci* 48:179–185. <https://doi.org/10.1248/jhs.48.179>
- Seller VT, Brilliant CD, Morgan C, Lewis SP, Duckers J, Boy FA, Lewis PD (2021) Anti-perspirant deodorant particulate matter temporal concentrations during home usage. *Build. Environ.* 195:107738. <https://doi.org/10.1016/j.buildenv.2021.107738>
- Seo Y, Seouk Park I (2013) Study for flow and mass transfer in toilet bowl by using toilet seat adopting odor/bacteria suction feature. *Build. Environ.* 67:46–55. <https://doi.org/10.1016/j.buildenv.2013.05.001>
- Srebric J, Chen Q (2002) Simplified numerical models for complex air supply diffusers. *HVACR Res.* 8:277–294. <https://doi.org/10.1080/10789669.2002.10391442>
- Szczepanik-Scislo N, Antonowicz A, Scislo L (2019) PIV measurement and CFD simulations of an air terminal device with a dynamically adapting geometry. *SN Appl. Sci.* 1:370. <https://doi.org/10.1007/s42452-019-0389-4>
- Tartarini F, Schiavon S, Cheung T, Hoyt T (2020) CBE thermal comfort tool: online tool for thermal comfort calculations and visualizations. *SoftwareX* 12:100563. <https://doi.org/10.1016/j.softx.2020.100563>
- Tung Y-C, Hu S-C, Tsai T-Y (2009) Influence of bathroom ventilation rates and toilet location on odor removal. *Build. Environ.* 44:1810–1817. <https://doi.org/10.1016/j.buildenv.2008.12.005>
- Tung Y-C, Shih Y-C, Hu S-C, Chang Y-L (2010) Experimental performance investigation of ventilation schemes in a private bathroom. *Build. Environ.* 45:243–251. <https://doi.org/10.1016/j.buildenv.2009.06.007>
- Wang Q, Liu L (2021) On the critical role of human feces and public toilets in the transmission of COVID-19: evidence from China. *Sustain Cities Soc* 75:103350. <https://doi.org/10.1016/j.scs.2021.103350>
- Wang J-X, Wu Z, Wang H, Zhong M, Mao Y, Li Y, Wang M, Yao S (2022) Ventilation reconstruction in bathrooms for restraining hazardous plume: Mitigate COVID-19 and beyond. *J. Hazard. Mater.* 439:129697. <https://doi.org/10.1016/j.jhazmat.2022.129697>
- Wang Q, Li Y, Lung DC, Chan P-T, Dung C-H, Jia W, Miao T, Huang J, Chen W, Wang Z, Leung K-M, Lin Z, Wong D, Tse H, Wong SCY, Choi GK-Y, Lam JY-W, To KK-W, Cheng VC-C, Yuen K-Y (2022) Aerosol transmission of SARS-CoV-2 due to the chimney effect in two high-rise housing drainage stacks. *J. Hazard. Mater.* 421:126799. <https://doi.org/10.1016/j.jhazmat.2021.126799>
- Wang C, Zhang X, Hu K, Liu Y (2023) Geometric-parameter influence and orthogonal evaluation on the thermal environment for an impinging jet ventilation system inlet. *Case Stud. Therm. Eng.* 51:103573. <https://doi.org/10.1016/j.csite.2023.103573>
- Wargocki P, Sundell J, Bischof W, Brundrett G, Fanger PO, Gyntelberg F, Hanssen SO, Harrison P, Pickering A, Seppänen O, Wouters P (2002) Ventilation and health in non-industrial indoor environments: report from a European Multidisciplinary Scientific Consensus Meeting (EUROVEN): Ventilation and health in non-industrial indoor environments. *Indoor Air* 12:113–128. <https://doi.org/10.1034/j.1600-0668.2002.01145.x>
- World Health Organization (2010) WHO guidelines for indoor air quality: selected pollutants. World Health Organization. Regional Office for Europe
- Yakhov V, Orszag SA, Thangam S, Gatski TB, Speziale CG (1992) Development of turbulence models for shear flows by a double expansion technique. *Phys. Fluids Fluid Dyn.* 4:1510–1520. <https://doi.org/10.1063/1.858424>
- Yang J-H, Kim O (2017) Improvement of ventilation efficiency by changing the shape of glass partition in bathroom of apartment house. *Indoor Built Environ.* 26:1274–1291. <https://doi.org/10.1177/1420326X16641313>
- Yu Ignatius TS, Yuguo Li, Wai Wong Tze, Wilson Tam, Chan Andy T, Lee Joseph HW, Leung Dennis YC, Tommy Ho (2004) Evidence of airborne transmission of the severe acute respiratory syndrome virus. *N Engl J Med* 350:1731–1739. <https://doi.org/10.1056/NEJMoa032867>
- Zhang T, (Tim), Li, P., Lin, C.-H., Wang, F., (2024) Modification of grilles to improve the lavatory environment on an aircraft. *Build. Environ.* 252:111246. <https://doi.org/10.1016/j.buildenv.2024.111246>

- Zhang B, Jiao L, Xu G, Zhao S, Tang X, Zhou Y, Gong C (2018) Influences of wind and precipitation on different-sized particulate matter concentrations (PM_{2.5}, PM₁₀, PM_{2.5–10}). *Meteorol. Atmospheric Phys.* 130:383–392. <https://doi.org/10.1007/s00703-017-0526-9>
- Zhang Z, Zeng L, Shi H, Liu H, Yin W, Gao J, Wang L, Zhang Y, Zhou X (2022) CFD studies on the spread of ammonia and hydrogen sulfide pollutants in a public toilet under personalized ventilation. *J. Build. Eng.* 46:103728. <https://doi.org/10.1016/j.jobe.2021.103728>
- Zhang J (2021) Infected in 14 seconds? How dangerous is the Delta variant? China Digital Science and Technology Museum. https://www.cdstm.cn/gallery/zhuanqi/ptzt/202108/t20210820_1054353.html. Accessed 20 Aug 2021
- Zhao B, Wu J (2009) Effect of particle spatial distribution on particle deposition in ventilation rooms. *J. Hazard. Mater.* 170:449–456. <https://doi.org/10.1016/j.jhazmat.2009.04.079>

Publisher's Note

Springer Nature remains neutral with regard to jurisdictional claims in published maps and institutional affiliations.